ELSEVIER

Journal of Materials Processing Technology 133 (2003) 84–89

Journal of Materials Processing Technology

www.elsevier.com/locate/jmatprotec

The effect of microstructure on the mechanical properties of two-phase titanium alloys

R. Filip*, K. Kubiak, W. Ziaja, J. Sieniawski

Department of Materials Science, Rzeszów University of Technology, ul. W. Pola 2, 35-959 Rzeszów, Poland

Abstract

This paper presents the results of investigations of the microstructure and mechanical properties of two-phase $\alpha + \beta$ titanium alloys after different heat treatment. The influence of the morphology of lamellar microstructure and phase composition on the tensile properties and fracture toughness of the alloys was studied. Static tensile, hardness and fracture toughness tests and microstructure investigations were performed. It was noticed that the cooling rate from the β-phase range and ageing conditions had an effect on the microstructure parameters, volume fraction and chemical composition of the β-phase, and has a significant effect on the mechanical properties of the alloys tested.

Keywords: Two-phase titanium alloys; Microstructure; Tensile properties; Fracture toughness

1. Introduction

The main factors determining the functional characteristics of two-phase titanium alloys are diffusion and diffusionless transformations taking place during heat treatment. The control of these processes by means of the selection of heat treatment conditions and chemical composition of the phases that are present in these alloys enables advancement in operational properties [1,2]. The mechanical properties of titanium alloys are important criteria of material service capabilities both in aerospace and industrial applications. The microstructure of the alloy is one of the important factors controlling its tensile properties, fatigue strength and fracture toughness [3–7]. The properties of titanium alloys can be varied over a wide range by heat treatment or thermomechanical treatment [6–9]. The microstructure of the alloy can be changed from equiaxial through bi-modal to fully lamellar. A bi-modal microstructure is reported to have advantages in terms of yield stress, tensile stress and ductility and fatigue stress. A fully lamellar structure is characterised by high fatigue crack propagation resistance and high fracture toughness. The important parameters for a lamellar structure with respect to mechanical properties are the β-grain size, size of the colonies of α-phase lamellae, thickness of the α-lamellae and the nature of the interlamellar interface (β-phase). Slow and intermediate cooling rates lead to a diffusion controlled nucleation and growth process of α-lamellae into the β-grains. A high cooling rates result in a martensitic transformation of the β-phase [10,11].

The aim of the present study was the determination of the relationship between processing conditions and alloy microstructure, and the effect of the morphology of the microstructure, the volume fraction and the chemical composition of the β-phase on the mechanical properties of two-phase titanium alloys. Therefore, to determine the influence of the morphology of the α- and β-phase on the strength properties of the alloy, two alloys were selected for the test: Ti–6Al–4V and Ti–6Al–2Mo–2Cr for which the coefficient of the β-phase stability is equal to $K_\beta = 0.3$ and 0.6, respectively. Mechanical tests were carried out using specimens made of material with a lamellar microstructure.

2. Materials and research methodology

The materials tested were high strength, two-phase $\alpha + \beta$ titanium alloys Ti–6Al–4V and Ti–6Al–2Mo–2Cr. The chemical composition of the alloys is presented in Table 1. The materials tested were vacuum melted and rolled in the $\alpha + \beta \rightarrow \beta$ temperature range in order to obtain a fine grained, equiaxial microstructure after stabilising annealing, which provides the best plasticity and high phase stability. A lamellar microstructure of α-phase was acquired in both alloys by means of proper cooling rates selection, which were specified on the basis of CCT diagrams. A different

* Corresponding author.

0924-0136/02/$ – see front matter
PII: S0924-0136(02)00248-0

Table 1
Chemical composition of Ti–6Al–4V and Ti–6Al–2Mo–2Cr alloys

Alloy	Stability factor, K_β	Alloying elements and impurities content (wt.%)										
		Al	Mo	V	Cr	Fe	C	Si	H	N	O	Ti
Ti–6Al–4V	0.3	6.1	–	4.3	–	0.16	0.01	–	0.015	0.06	0.12	Balance
Ti–6Al–2Mo–2Cr	0.6	6.3	2.6	–	2.1	0.40	0.05	0.2	0.016	0.016	0.09	Balance

value of prior β-phase diameter was obtain as a result of different times of heating at the β-phase range (from 40 to 120 min).

Dilatometric test was performed employing absolute dilatometer LS-4 in order to determine the influence of cooling rate on the temperature of $\alpha + \beta \rightarrow \beta$ phase transformations, kinetics of phase transformations during continuous cooling and morphology of the two-phase $\alpha + \beta$ microstructure. Changes in specimens elongation were measured by means of an inductive converter and *X*–*Y* recorder Riken Denshi. Temperature was measured using a Ni–CrNi thermocouple. Rounded specimens 4 mm in diameter and 15 mm long with $\varnothing 1.6 \times 7.5$ hole for a thermocouple were used for the tests. A protective argon atmosphere was applied.

The Ti–6Al–2Mo–2Cr alloy was heat treated before fracture toughness tests in order to determine the influence of α-phase morphology on its fracture toughness. Heat treatment was conducted in an electric chamber furnace in a protective argon atmosphere. It consisted of solution treatment at a temperature of 1055 K for 1 and 2 h, followed by oil quenching for 1.5 h followed by water cooling and ageing at a temperature of 623, 723 or 823 K for 5 and 20 h. Specimens were air cooled after ageing.

Mechanical testing of the specimens with lamellar microstructure were performed. Hardness tests were carried out using a Vickers hardness tester with the load of 980 N. A static tensile test was carried out on the UTS-100 testing machine. The specimens were of cylindrical shape. During the test the strain rate $\varepsilon = 0.005\ \mathrm{s}^{-1}$ was applied. Four specimens in each series were examined and average values of mechanical properties were determined. Ultimate tensile strength R_m, 0.2% proof stress $R_{0.2}$, reduction in area Z and elongation A_5 were measured.

Fracture toughness three point bending tests of Ti–6Al–2Mo−2Cr alloy were conducted in accordance with ASTM E 399 standard [12] using single edge notched bend specimens. The specimen had a thickness $B = 10$ mm, width $W = 20$ mm and loading span $l = 80$ mm, providing plane-strain conditions at the notch tip. The notch was cut to 9 mm length using a grinding wheel. To precisely localise the fatigue crack, the notch tip was cut with a wire saw (wire of 0.1 mm diameter). Specimens were fatigue pre-cracked to a crack depth of 1.25 mm using a pulsator with load frequency of 20 Hz. Load–displacement curves of type III were obtained and used for K_{Ic} determination. Fracture toughness K_{Ic} was calculated using the following formula:

$$K_{Ic} = \frac{P_Q l}{BW^{3/2}} f\left(\frac{a}{W}\right)$$

where P_Q is the critical load determined from the load–displacement curve, B the specimen thickness, W the specimen width $= 2B$, l the loading span $= 4W$, a the crack length and $f(a/W)$ the dimensionless function of a/W [12].

The microstructure of the specimens was examined using an optical microscope Neophot 2. Quantitative analysis of α phase morphology was carried out on a Quantimet 720 image analysis system. The specimens were ground, polished and etched at 270 K in two reagents having the following compositions: 10 ml KOH (40%) + 5 ml H_2O_2 + 20 ml H_2O and 1 ml HF + 30 ml HNO_3 + 30 ml H_2O_2. The second etching was carried out for contrast enhancement. The following quantities were determined: V_v—volume fraction of α-phase, D_β—diameter of the primary β-phase grains, D_α—size of equiaxial α-grains, d—size of colonies of α-lamellae, t—thickness of α-lamellae.

The fracture surfaces of the specimens after static tensile tests and fracture toughness tests were observed using a scanning electron microscope Novascan 30 with 7 nm resolution at 15 kV acceleration voltage. Fractographic examinations were indispensable for analysis of the damage process.

3. Results and their analysis

The microstructure of the alloys tested after cooling at a controlled cooling rate (lamellar) is presented in Figs. 1 and 2. It was noticed that the thickness and length of the α-phase decrease with increasing cooling rate and with increasing content of the β-stabilising elements. A typical microstructure of the Ti–6Al–2Mo−2Cr alloy after the heat treatment applied in the study is shown in Fig. 3.

As a result of dilatometric examination the $\beta \rightarrow \alpha + \beta$ phase transformation temperature was determined, particularly the start and finish temperature of the metastable phase decomposition and the temperature ranges of martensitic phases $\alpha'(\alpha'')$ presence. The microstructure obtained while cooling with different rates was identified. The range of cooling rate for the development of lamellar α-phase was determined as a result of X-ray structural

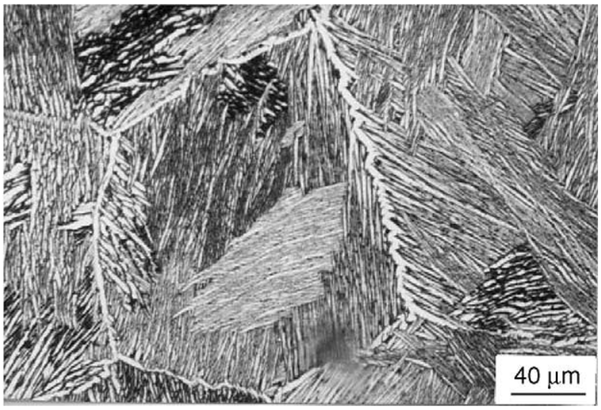

Fig. 1. Microstructure of the Ti–6Al–4V alloy after cooling in air, with α-phase lamellae in the β-matrix.

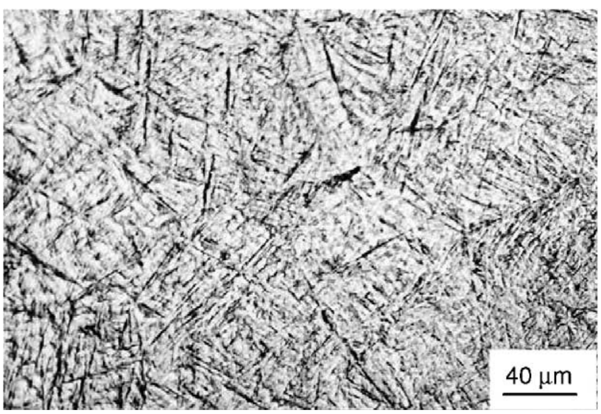

Fig. 2. Microstructure of the Ti–6Al–4V alloy after cooling in water showing $\alpha'(\alpha'')$ martensitic plates.

analysis. Continuous cooling of Ti–6Al–4V and Ti–6Al–2Mo–2Cr alloys from the β-phase range leads to the development of a microstructure composed both of martensitic phases $\alpha'(\alpha'')$ and stable α- and β-phase at cooling rate $v_c = 1.2{-}40\ \mathrm{K\,s^{-1}}$, and stable lamellar microstructure $\alpha + \beta$ at cooling rate $v_c < 1.2\ \mathrm{K\,s^{-1}}$ (Table 2).

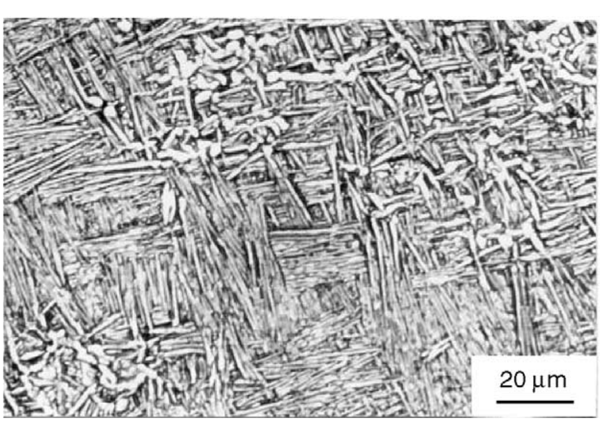

Fig. 3. Microstructure of Ti–6Al–2Mo–2Cr alloy; 1055 K/1 h/oil+825 K/5 h.

Table 2
Phase composition of Ti–6Al–4V and Ti–6Al–2Mo–2Cr alloys after cooling with controlled cooling rates

Cooling rate ($\mathrm{K\,s^{-1}}$)	Phase composition	
	Ti–6Al–4V	Ti–6Al–2Mo–2Cr
48	$\alpha'(\alpha'')$	$\alpha'(\alpha'')$
40	$\alpha'(\alpha'')$	$\alpha'(\alpha'')$
18	$\alpha'(\alpha'')$	$\alpha'(\alpha'')$
9	$\alpha + \alpha'(\alpha'')$	$\alpha + \alpha'(\alpha'') + \beta$
7	$\alpha + \alpha'(\alpha'')$	$\alpha + \alpha'(\alpha'')_{\mathrm{trace}} + \beta$
3.5	$\alpha + \alpha'(\alpha'')_{\mathrm{trace}} + \beta$	$\alpha + \alpha'(\alpha'')_{\mathrm{trace}} + \beta$
1.2	$\alpha + \beta$	$\alpha + \beta$
0.08	$\alpha + \beta$	$\alpha + \beta$
0.04	$\alpha + \beta$	$\alpha + \beta$
0.024	$\alpha + \beta$	$\alpha + \beta + TiCr_2$
0.008	$\alpha + \beta$	$\alpha + \beta + TiCr_2$
0.004	$\alpha + \beta$	$\alpha + \beta + TiCr_2$

The tensile properties of the alloys are presented in Figs. 4 and 5. The yield stress of the alloys tested increases monotonously due to the continuous refinement of the lamellar microstructure. Then the slip length across α-plate colonies is reduced. The highest tensile elongation was obtain at intermediate cooling rates ($9\ \mathrm{K\,s^{-1}}$), due to two effects: an increase in ductility by the reduction of slip length, and an decrease in ductility by a conversion to an intergranular fracture mode.

Fractographic examination of the fracture surfaces of the alloys showed that the material with large grain size displays intergranular faces with dimensions corresponding to the grain size. For the fine grained material the grain boundary fracture is greatly reduced (Fig. 6). In Ti–6Al–2Mo–2Cr alloy zones of large plastic deformation can be seen in β-phase regions and propagating crack passes round the colonies of parallel α-phase lamellae (Fig. 7).

The dependence of the geometrical parameters of the α-phase in Ti–6Al–2Mo–2Cr alloy on heat treatment conditions is shown in Figs. 8 and 9. The influence of α-phase

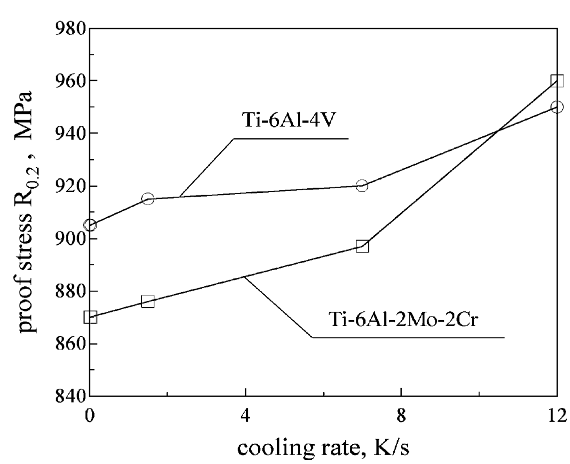

Fig. 4. Effect of the cooling rate on the proof stress of Ti–6Al–4V and Ti–6Al–2Mo–2Cr alloys.

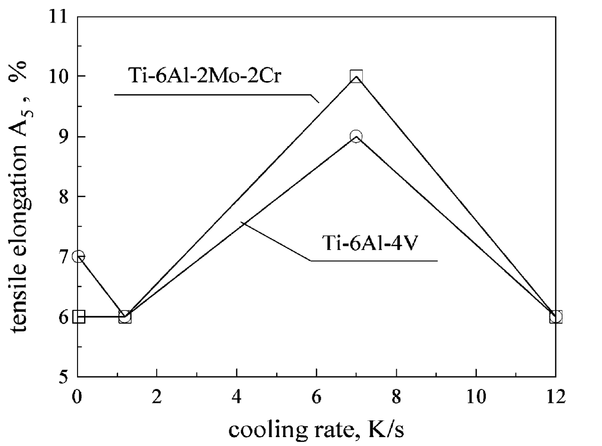

Fig. 5. Effect of cooling rate on the tensile elongation of Ti–6Al–4V and Ti–6Al–2Mo–2Cr alloys.

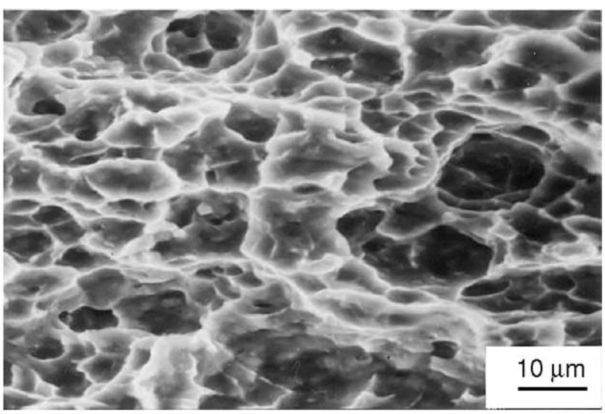

Fig. 6. Fracture surface of Ti–6Al–4V alloy after the tensile test.

morphology on the fracture toughness of this alloy is shown in Figs. 10 and 11.

The highest fracture toughness of Ti–6Al–2Mo–2Cr alloy, about 92.8 MPa m$^{1/2}$, was obtained for specimens solutionised at 1055 K (lower part of temperature range of $\alpha + \beta \rightarrow \beta$ phase transformation) for 1 h, quenched in oil and aged at 623 K for 5 h. The lowest fracture toughness,

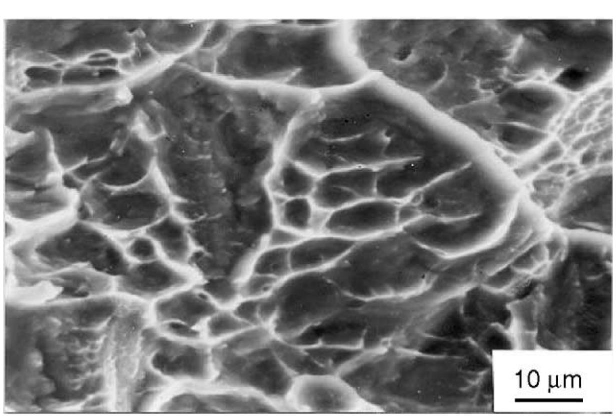

Fig. 7. Fracture surface of Ti–6Al–2Mo–2Cr alloy after the tensile test.

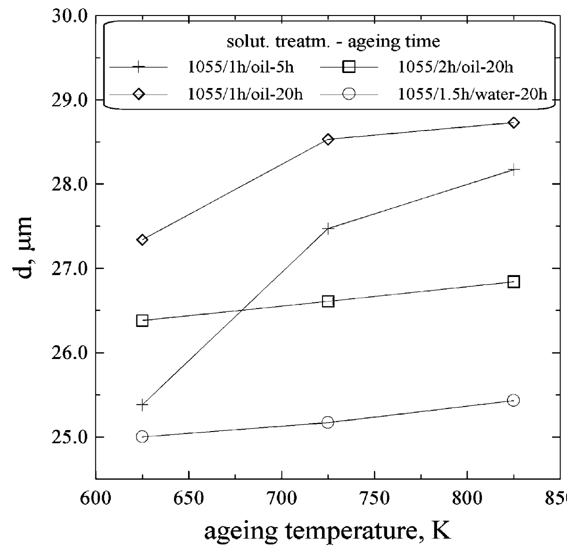

Fig. 8. The effect of heat treatment conditions of Ti–6Al–2Mo–2Cr alloy on the size (d) of the colony of α-lamellae.

about 51.3 MPa m$^{1/2}$, was obtained for specimens solutionised at 1055 K for 2 h, quenched in oil and aged at 823 K for 20 h.

Regardless of differences in K_{Ic} values, the fracture surfaces of all specimens had a similar appearance (Fig. 12) which indicates that the fracture mechanism was similar and failure was characterised by rapid, unstable propagation of a running ductile crack.

The fracture toughness of the alloy is controlled by the size of colonies of lamellar α-phase, thickness of α-lamellae and size of equiaxial α-phase grains. An increase of both ageing temperature (from 623 to 823 K) and time (up to 20 h) decreases the fracture toughness of the examined alloy. At higher ageing temperatures, the process of metastable

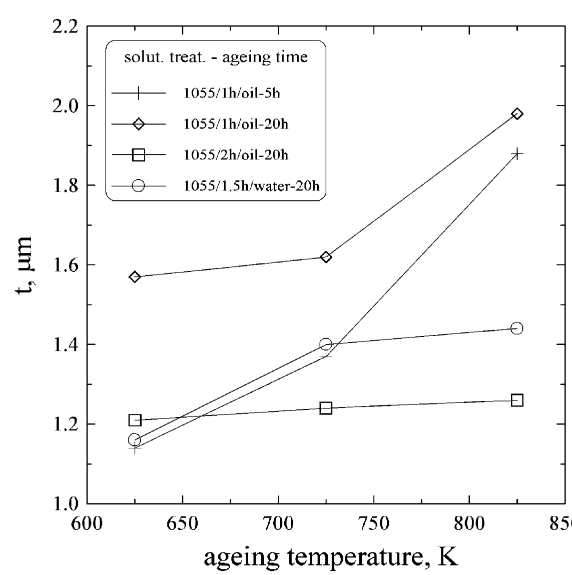

Fig. 9. The effect of heat treatment conditions of Ti–6Al–2Mo–2Cr alloy on the thickness (t) of α-lamellae.

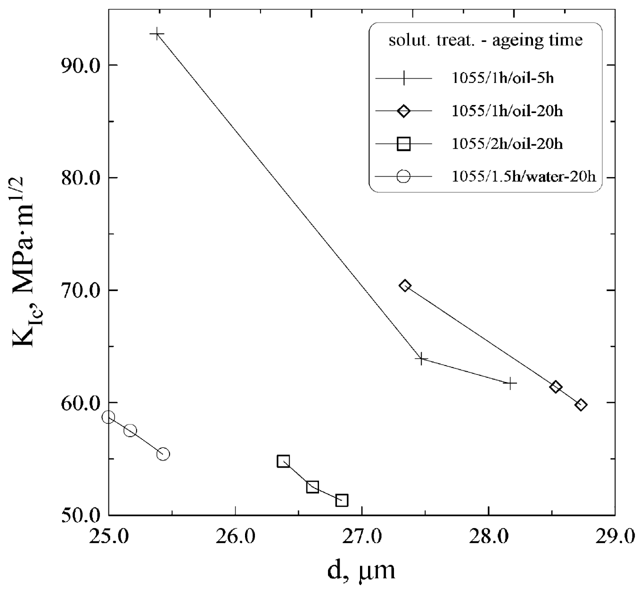

Fig. 10. The effect of the size (d) of the colony of α-lamellae on the fracture toughness of Ti–6Al–2Mo–2Cr alloy.

phases decomposition is faster and results in increased size of α lamellae colonies, increased thickness of α-lamellae and growth of equiaxial α-phase grains. After it is completed, coagulation of phase transformation products takes place, leading to significant reduction of fracture toughness and an increase of alloy plasticity.

The fracture toughness is improved with increasing the amount of the lamellar α-phase. Colonies of α-phase lamellae with various orientations hinder the crack growth. When crossing the boundary between colonies, the crack changes direction, which causes crack branching and secondary crack creation. These processes require additional energy

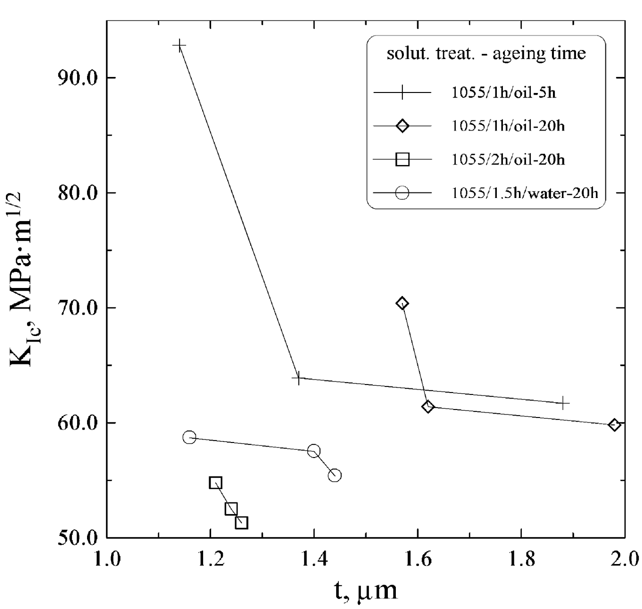

Fig. 11. The effect of the thickness (t) of α-lamellae on the fracture toughness of Ti–6Al–2Mo–2Cr alloy.

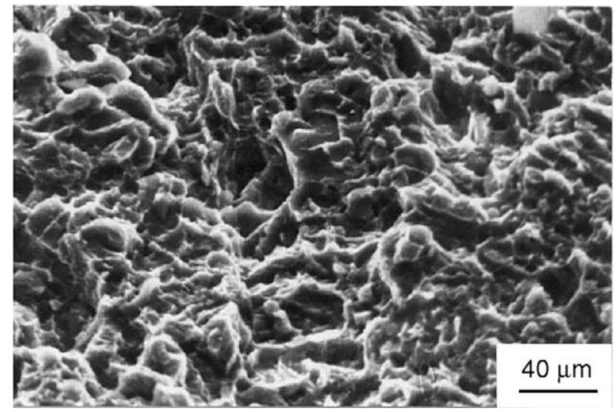

Fig. 12. The fracture surface of Ti–6Al–2Mo–2Cr alloy after the fracture toughness test.

and result in increased fracture toughness of the material. Crack propagation through equiaxial α-phase grains does not require so much energy, as crack branching is absent and in turn the fracture toughness is reduced.

4. Summary

The studies carried out have established that the geometrical parameters of the microstructure are influenced by the cooling rate from the β-phase field and the heat-treatment conditions, i.e. the cooling rate from the solution treatment temperature and the ageing time and temperature.

A low cooling rates lead to a diffusion controlled growth process of α-phase lamellae, and neighbouring α- and β-lamellae possess highly coincident interfaces. A high cooling rates results in a martensitic transformation, and difference in the crystallographic orientation of adjacent lamellae is considerably larger, resulting in interfaces with low coincidence. It is to be noted that the proof stress increases due to continuous refinement of the microstructure, reducing the slip length. The tensile elongation shows a maximum at intermediate cooling rates. This is the result of two effects: the reduction of slip length and a transition to an intergranular fracture mode.

The fracture toughness of Ti–6Al–2Mo–2Cr alloy can be increased by adjusting the microstructure, i.e. the amount and size of lamellar and equiaxial α-phase, through proper heat treatment. Increase in the ageing temperature (from 623 to 823 K) and time (up to 20 h) decreases the fracture toughness of the Ti–6Al–2Mo–2Cr alloy due to increase of the geometrical parameters of the lamellar and equiaxial α-phase. Increase in the volume fraction of the equiaxial α-phase during ageing leads to fracture toughness reduction.

Acknowledgements

This work was supported by the KBN under Grant 7 T08A 03809.

References

[1] D. Eylon, S. Fujishiro, P.J. Postans, F.H. Froes, J. Met. 36 (1984) 55–61.

[2] S. Sastry, T.C. Peng, P.J. Mechter, J.E. O'Neal, J. Met. 36 (1984) 21–28.

[3] V.J. Colagelo, F.A. Heizer, Analysis of Metallurgical Failures, Wiley, New York, 1987.

[4] J.D. Emburg, F. Zok, Micromechanisms of fracture, in: Proceedings of the 26th Conference of Metallurgists—Winnipeg 1987, Pergamon Press, New York, 1988.

[5] J. Sieniawski, Scientific papers of the Rzeszow University of Technology—Mechanics No. 10, Rzeszow, 1985 (in Polish).

[6] L.J. Hunter, M. Strangwood, P. Bowen, in: P.A. Blenkinsop, W.J. Evans, H.M. Flower (Eds.), Effect of Microstructure on the Fracture Behaviour of the $\alpha + \beta$ Titanium Alloy Ti–4Al–4Mo–2Sn–0.5Si wt.% (IMI 550), Titanium'95: Science and Technology, The Institute of Materials, London, 1996, p. 925.

[7] J. Sieniawski, The effect of phase composition on the fracture toughness (K_{Ic}) of structural titanium alloys, in: Proceedings of the ISUMEL-2 Second International Symposium of Ukrainian Mechanical Engineers in Lviv, Lviv, 1995, p. 101.

[8] G. Lütjering, Influence of processing on microstructure and mechanical properties of $\alpha + \beta$ titanium alloys, Mater. Sci. Eng. A 243 (1998) 32.

[9] W.J. Evans, Optimising mechanical properties in $\alpha + \beta$ titanium alloys, Mater. Sci. Eng. A 243 (1998) 89.

[10] M. Peters, G. Lütjering, in: Proceedings of the Titanium'80: Science and Technology, TMS, 1990, pp. 925–935.

[11] G. Lütjering, J. Albrecht, O.M. Ivasishin, in: Proceedings of the Titanium'95: Science and Technology, TMS, 1995, pp. 1163–1170.

[12] E 399-83, Standard Test Method for Plane-strain Fracture Toughness of Metallic Materials, ASTM, Philadelphia, 1983.